Journal of Virological Methods 173 (2011) 75–84

Contents lists available at ScienceDirect

Journal of Virological Methods

journal homepage: www.elsevier.com/locate/jviromet

Highly sensitive capacitive biosensor for detecting white spot syndrome virus in shrimp pond water

Saluma Samanman[a,b,c], Proespichaya Kanatharana[a,b,c], Wilaiwan Chotigeat[d], Panchalika Deachamag[d], Panote Thavarungkul[a,b,e,*]

[a] Trace Analysis and Biosensor Research Center, Prince of Songkla University, Hat Yai, Songkhla 90112, Thailand
[b] Center for Innovation in Chemistry, Faculty of Science, Prince of Songkla University, Hat Yai, Songkhla 90112, Thailand
[c] Department of Chemistry, Faculty of Science, Prince of Songkla University, Hat Yai, Songkhla 90112, Thailand
[d] Center for Genomics and Bioinformatics Research, Faculty of Science, Prince of Songkla University, Hat-Yai, Songkhla 90112, Thailand
[e] Department of Physics, Faculty of Science, Prince of Songkla University, Hat Yai, Songkhla 90112, Thailand

Article history:
Received 4 October 2010
Received in revised form
21 December 2010
Accepted 10 January 2011
Available online 21 January 2011

Keywords:
White spot syndrome virus
Affinity biosensor
Trace analysis
Shrimp pond water
Capacitance

A B S T R A C T

Water is one major pathways by which the white spot syndrome virus (WSSV) pathogen enters aquaculture facilities. This paper describes the production and use of a capacitive biosensor for the quantitative detection of as little as 1 copy/μl of WSSV in shrimp pond water. A glutathione-S-transferase tag for white spot binding protein (GST-WBP) was immobilized on a gold electrode through a self-assembled monolayer. Binding between WSSV and the immobilized GST-WBP was directly detected by a capacitance measurement. Under optimum conditions, the capacitive biosensor detected WSSV over a wide linear range of between 1 and 1×10^5 copies/μl. The system was highly selective for WSSV. One analysis cycle required only 20–25 min of analysis time and 25 min of regeneration time. The capacitive biosensor was applied to analyze WSSV concentration in eight shrimp pond water samples and the results were in good agreement with those obtained by a real time quantitative polymerase chain reaction (real-time PCR) method ($P > 0.05$). The immobilized GST-WBP provided and could be reused for up to 39 analysis cycles for one electrode preparation with a relative standard deviation (RSD) of 2.4% and a good reproducibility of residual activity ($95.8 \pm 2.3\%$). The appealing performance of this biosensor indicated that it had great potential for an accurate very sensitive, quantitative, detection method for WSSV.

1. Introduction

Shrimp cultivation has been a major industry of Thailand since the late 1980s (Flegel, 2006). The industry employs about one million people nationwide, and exports about US$2 billion of shrimp per year (Flegel, 2006; Tanticharoen, 2008). However, the cultivation and exportation of shrimp has been affected by infectious outbreaks of white-spot syndrome virus (WSSV) (Tanticharoen, 2008) that can cause high mortality rates, reaching 100% within 3–10 days (Lightner, 1996; Chen et al., 2002).

A number of diagnostic tools have been used to detect WSSV. Qualitative methods include conventional polymerase chain reaction (PCR) (Lo et al., 1996; Esparza-Leal et al., 2009), in situ hybridization (ISH) and immunological methods (Chen et al., 2002; Wang and Zhan, 2006). Quantitative methods, include real-time polymerase chain reaction (real-time PCR) (Tan et al., 2001; Dhar et al., 2001; Sritunyalucksana et al., 2006; Yuan et al., 2007) and real-time loop-mediated isothermal amplification (RT-LAMP) (Kono et al., 2004). However, these assays are quite expensive, require many steps as well as an expert operator (Rajendran et al., 2005; Mekata et al., 2009). In addition, these methods have been mainly used for the detection of WSSV in shrimp tissues, carrier animals and sediments (Lightner, 1996; Hossain et al., 2001, 2004; Hameed et al., 2005; Natividad et al., 2008). However the major pathway of WSSV entering the aquaculture facilities is by water (Cohen et al., 2005; Quang et al., 2009) and at present there are no treatments available to control the disease, except perhaps for expensive water filtration and disinfection methods (Lightner, 2005). Therefore, a sensitive, specific and rapid method to detect WSSV in water would be very useful for the detection of WSSV contamination before stocking ponds and to monitor the WSSV spread during shrimp cultivation. To fulfill these requirements the label-free capacitive affinity biosensor based on potential step perturbation is an interesting approach.

The principle of this potentiostatic step capacitive biosensor is based on the electrical double-layer theory. An electrode at which

* Corresponding author at: Department of Physics, Faculty of Science, Prince of Songkla University, Hat Yai, Songkhla 90112, Thailand.
Tel.: +66 74 288753, fax: +66 74 558849.
E-mail address: panote.t@psu.ac.th (P. Thavarungkul).

0166-0934/$ – see front matter © 2011 Elsevier B.V. All rights reserved.
doi:10.1016/j.jviromet.2011.01.010

no charge transfer can occur across the metal–solution interface when the potential across it is changed can be represented by a capacitor (Bard and Faulkner, 2001). Charged species and dipoles of the solution will be oriented at the electrode–solution interface making up the electrical double-layer (Berggren et al., 2001). The binding of the analyte to the immobilized recognition element on the electrode surface leads to a thicker dielectric layer on the electrode–solution interface (Gebbert et al., 1992) pushing the ions and water molecules further from the electrode surface and causing the capacitance to decrease (Berggren et al., 2001). This capacitive biosensor, using potential step perturbation has been successfully applied as a sensitive technique for the direct detection of affinity reaction, such as antibody–antigen (Berggren and Johansson, 1997; Mirsky et al., 1997; Hedstrom et al., 2005; Limbut et al., 2006; Loyprasert et al., 2008; Suwansa-ard et al., 2009), protein–DNA (Numnuam et al., 2009) and protein–heavy metal ions (Bontidean et al., 1998). This relative low cost electrochemical detection system can provide a low detection limit and high sensitivity.

To detect WSSV, a biorecognition element that is specific to this virus is required. At the Center for Genomics and Bioinformatics Research, Faculty of Science, Prince of Songkla University, Hat-Yai, Songkhla, Thailand, a white spot binding protein (WBP) that can bind specifically to the VP26 envelope protein on WSSV has been cloned from a WSSV infected black tiger shrimp (*Penaeus monodon*) (Youtong et al., 2011). Due to the short amino acid sequence of the WBP (MW = 3 kDa), it was fused to glutathione-S-transferase (GST, MW = 29 kDa) and is called glutathione-S-transferase tag white spot binding protein (GST-WBP, MW = 32 kDa). This GST-WBP would be a good recognition element for the affinity detection of WSSV.

In the present work, the proposed capacitive biosensor system was used to detect WSSV present in trace amounts by immobilizing GST-WBP on a self-assembled thiourea monolayer, modified gold electrode. Parameters affecting the response of the detection system were first optimized. Under optimum conditions, the capacitive biosensor system was applied to determine the amount of WSSV in water from real shrimp cultivation ponds and the results were compared with those obtained by real-time PCR.

2. Materials and methods

2.1. Materials

Glutathione-S-transferase tag white spot syndrome virus binding protein (GST-WBP), white spot syndrome virus (WSSV) and yellow head virus (YHV) stock solution were provided by the Center for Genomics and Bioinformatics Research, Faculty of Science, Prince of Songkla University, Hat Yai, Songkhla, Thailand. The viral titer (8.5×10^7 copies/μl) was determined by real-time PCR. Thiourea and glutaraldehyde were purchased from Sigma–Aldrich (Steinheim, Germany), and Fluka (Buchs, Switzerland), respectively. 1-Dodecanethiol was obtained from Aldrich (St. Louis, USA). All other chemicals were of analytical grade. All buffers were prepared with deionized water treated with a reverse osmosis-deionized system (Millipore, Bedford, USA). Before use, buffers were filtered through a nylon membrane filter (Albet, Spain, pore size 0.20 μm) with subsequent degassing.

2.2. Immobilization of GST-WBP

A gold electrode (diameter 3.0 mm, 99.99% purity) was polished (Gripo® 2V, Metkon Instruments Ltd., Bursa, Turkey) using alumina slurries (Metkon, Bursa, Turkey) with particle diameters 5.0, 1.0 and 0.3 μm, respectively. It was then cleaned through sonication in ethanol for 1 min and deionized water for 10 min, then by electrochemical etching in 0.5 M H_2SO_4 using a potential from 0 to 1.5 V vs. an Ag/AgCl reference electrode (Metrohm, Herisau, Switzerland) with a scan rate of 0.1 V/s for 25 scans. The electrode was then dried with pure nitrogen gas.

One of the important requirements of the proposed capacitive system is that the electrode surface needs to be insulated. If the modified electrode is not isolated, it can induce a false-positive signal (Wongkittisuksa et al., 2011). A self-assembled monolayer (SAM) is one of the methods widely used for preparation of an insulated surface. The cleaned gold electrode was immersed in 250 mM thiourea solution at room temperature for 24 h (Limbut et al., 2006) then thoroughly rinsed with deionized water. During this time the thiourea self-assembled onto the electrode surface. The modified electrode was then treated with 5% (v/v) glutaraldehyde in 10 mM of sodium phosphate buffer pH 7.00 at room temperature for 20 min to activate the aldehyde groups, rinsed with deionized water and dried with nitrogen gas. Twenty microliters of 150 μg/ml GST-WBP was placed on the electrode surface and left overnight at 4 °C for the binding between the GST-WBP NH_2-terminal and the activated aldehyde groups. The electrode was then rinsed with 10 mM Tris–HCl, pH 7.00 before immersing it in 1.0 M ethanolamine pH 8.50 for 7 min to block any remaining reactive sites of the aldehyde groups that were not coupled with the GST-WBP. This was followed by immersing the electrode in 10 mM 1-dodecanethiol ethanolic solution for 20 min to block any pinholes on the electrode surface.

2.3. Capacitance measurement

A flow injection capacitance measurement system was set-up as shown in Fig. 1. The modified gold electrode (working electrode), stainless steel tube (auxiliary electrode) and a custom made Ag/AgCl (reference electrode) were placed in a custom-made measuring flow cell (10 μl) and they were connected to a potentiostat (Model EA161, EDAQ, New South Wales, Australia). In this potentiostatic step capacitive system the non-faradaic signal is monitored. Since the electrode surface is totally insulated the system acts like a simple RC circuit (Fig. 2(a)). The capacitance measurement was performed by applying 50 mV potential step pulses (pulse width 6.4 ms) on the working electrode, one pulse per min (Fig. 2(b)). Although the charge does not cross the interface, the transient external current can flow (Bard and Faulkner, 2001). This transient current response (Fig. 2(c)) can be described by Eq. (1):

$$i(t) = \frac{u}{R_s} \exp\left[\frac{-t}{R_s C_{total}}\right] \quad (1)$$

where $i(t)$ is the current response expressed as a function of time, u the pulse potential applied, R_s is the electrical resistance of elements serially connected to the layer, t the time elapsed after the potential step was applied, and C_{total} is the total capacitance measured at the working electrode/solution interface (Berggren et al., 2001; Jiang et al., 2003). Eq. (2) was obtained by taking the logarithm of Eq. (1)

$$\ln i(t) = \ln \frac{u}{R_s} - \frac{t}{R_s C_{total}} \quad (2)$$

C_{total} and R_s could then be calculated from the slope and intercept of the linear least-square fitting of ln $i(t)$ vs. t (Fig. 2(d)). The obtained capacitance (C_{total}) of each current response was then plotted as a function of time, one per min (Fig. 2(e)).

For a typical analysis the running buffer was first injected to obtain the baseline capacitance (Fig. 2(e)). When WSSV was injected it bound to the immobilized GST-WBP resulting in a decrease of C_{total} (Figs. 1 inset and 2(e)). The capacitance change (ΔC) that corresponded to the concentration of WSSV could then be obtained from the measured capacitance before ($C_{GST\text{-}WBP}$) and

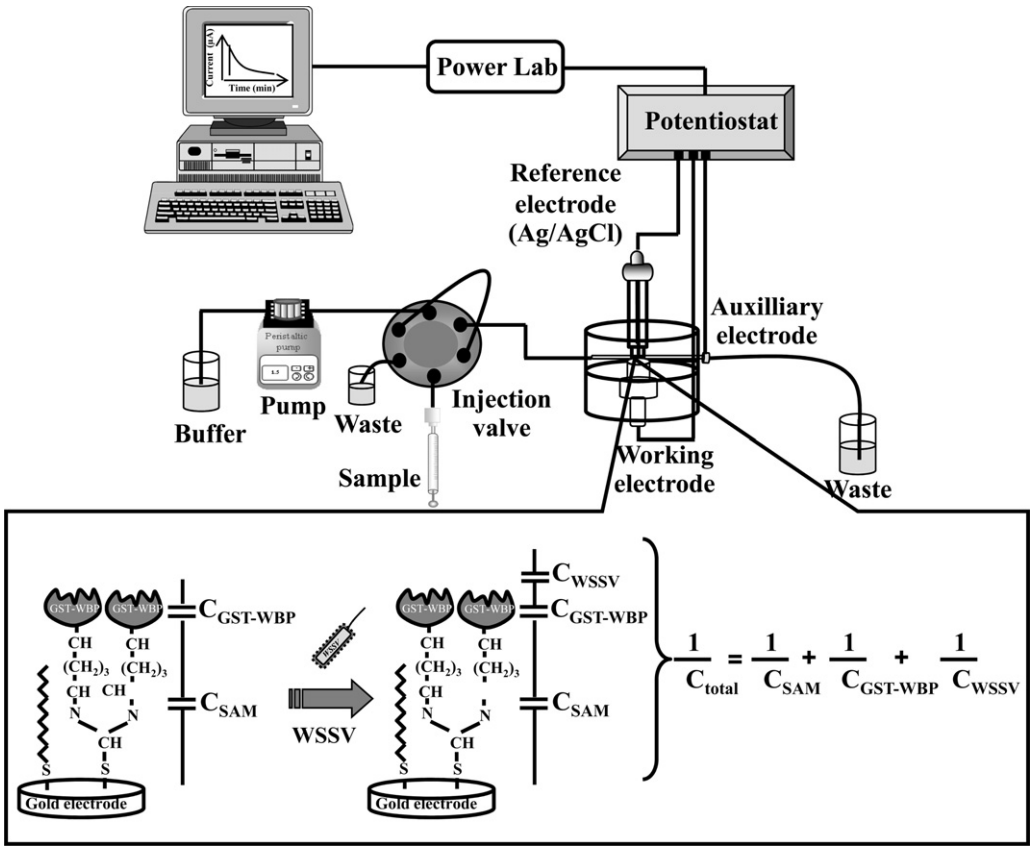

Fig. 1. Schematic diagram of the flow injection capacitive biosensor system. GST-WBP was immobilized on the electrode surface via SAM of thiourea and the remaining pinholes on the electrode surface were blocked with 1-dodecanthiol. The total capacitance measured at the working electrode/solution interface (C_{total}) is from C_{SAM}: the capacitance of the self-assembled thiourea monolayer, $C_{GST-WBP}$: the capacitance of the immobilized GST-WBP and C_{WSSV}: the capacitance of the WSSV analyte interaction (modified from Numnuam et al., 2009).

after ($C_{GST-WBP, WSSV}$) the binding between GST-WBP and WSSV (Eq. (3)).

$$\Delta C = C_{GST-WBP,WSSV} - C_{GST-WBP} \quad (3)$$

Then, a regeneration solution was injected to break the binding between the immobilized GST-WBP and WSSV followed by a continuous flow of running buffer that returned the capacitance to the baseline for a new measurement.

2.4. Optimization and performance of the capacitive system

The operating conditions (Table 1) of the flow injection capacitive biosensor system were optimized. Studied parameters were: the composition, pH, and concentration of the regeneration solution, the pH and concentration of the running buffer, flow rate and sample volume. The optimization was performed by changing a single parameter while keeping other parameters constant. Each tested value was carried out in triplicate. The optimum value was chosen by keeping a balance between a high response and a short analysis time. The regeneration solution was the first parameter optimized followed by the running buffer, sample volume and flow rate, respectively, using 100 copies/μl of the WSSV standard. Using the optimum conditions, the capacitive biosensor system performance such as its linear range and limit of detection were studied.

2.5. Determination of WSSV in pond water used for shrimp cultivation

Shrimp pond water samples were collected from eight different cultivation ponds in three provinces. One from Satun, another from Songkhla, and six others from Surat Thani, Thailand. All samples were analyzed by the flow injection capacitive biosensor system under optimum conditions. The same samples were also tested with a quantitated real-time PCR (COBAS Tag Man 48, Roche, USA). Real-time PCR in a 25 μl reaction containing 12.5 μl of iQ™SYBR®Green Supermix (Roche, Germany), 20 pmol of each primer and 1 μl of supernatant solution was performed by using the fluorescence detection Mx3000P™ (Stratagene, La Jolla, CA). The primer was designed from the shrimp white spot syndrome virus isolate Japan 98 VP19 gene, GenBank accession number AY249447.1. The forward primer and reverse primer were VP19-FB: 5′CGGGATCCATGGCCACCACGACT AA3′, VP19-RX: 5′GCCTCGAGCCTGATGTTGTGTTTTCTATA3′ respectively. The PCR was performed according to Youtong et al., 2011. PCRs were conducted with the initial denaturation step at 95 °C for 5 min, followed by 40 cycles of 94 °C for 0.3 min, 59 °C for 1 min and 72 °C for 1 min. The standard curve for quantification of the VP19 gene was prepared using serial dilutions of the linearized purified PCR product of the VP19 gene. The dynamic range of detection was determined by preparing 10-fold serial dilutions of the VP19 gene in the range of 1×10^9–1×10^1 copies/μl and used as a standard curve for quantification of the WSSV concentration.

3. Results

3.1. Electrochemical characterization of the modified gold electrode

Insulation of the electrode surface is an important condition of the proposed capacitive system and the degree of insulation of the

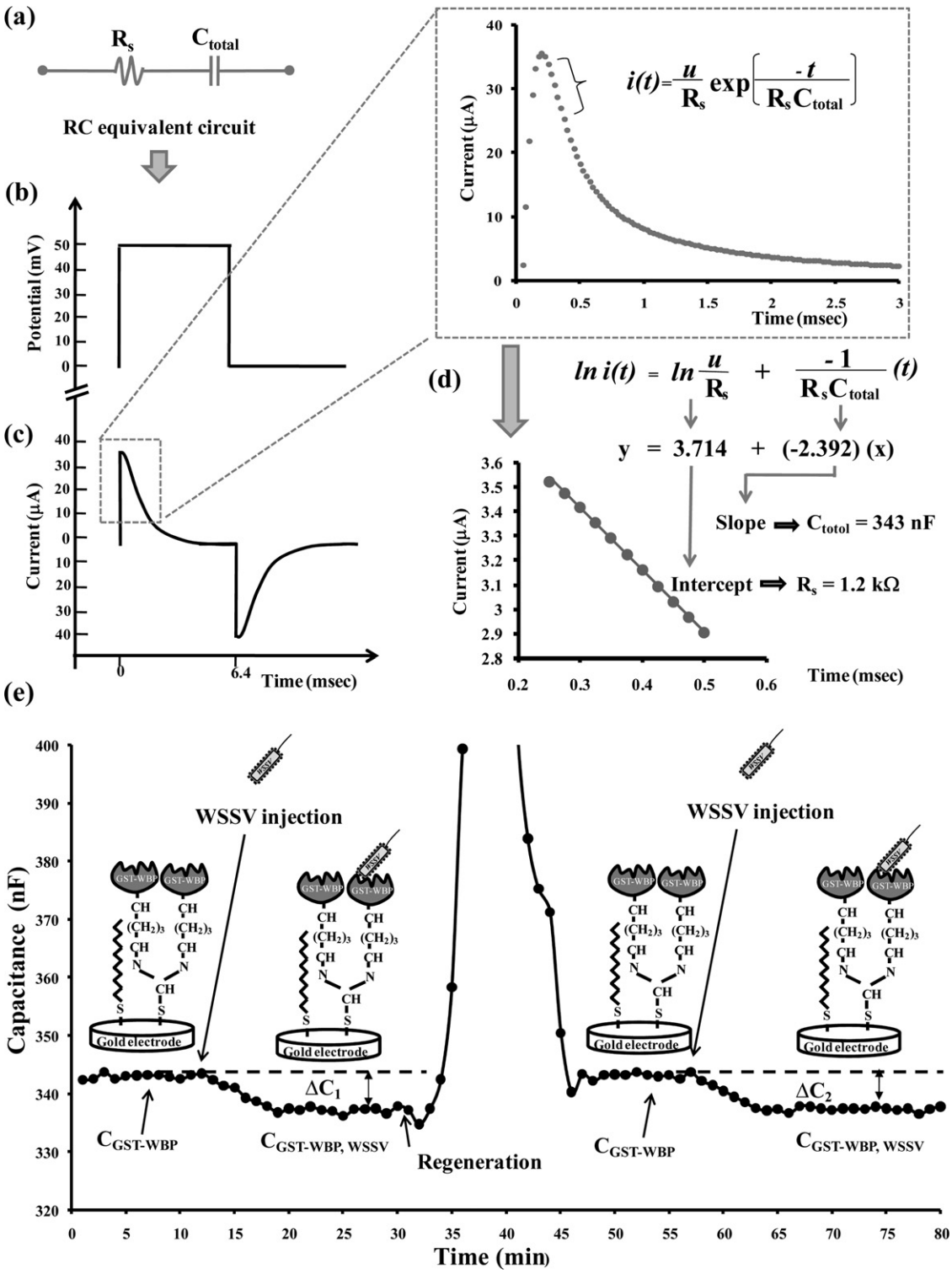

Fig. 2. Capacitance measurement. (a) The system can be represented by an RC equivalent circuit consisting of the electrical resistance of elements serially connected to the layer (R_s) and the total capacitance measured at the working electrode/solution interface (C_{total}). (b) The potential step pulse with a 0 mV initial potential and an amplitude of 50 mV (one per minute, pulse width = 6.4 ms) was applied to the working electrode (vs. a Ag/AgCl reference electrode). (c) The obtained transient current decayed exponentially as described by the equation. (d) Taking the logarithm of the equation C_{total} and R_s could be obtained from the slope and intercept of the linear least-square fitting of ln $i(t)$ vs. t. (e) The obtained C_{total} of each pulse was then plotted as a function of time. A baseline capacitance ($C_{GST-WBP}$) was first obtained by passing through the running buffer (30 μl/min). When standard WSSV (300 μl, 100 copies/μl) was injected into the continuous flow buffer, the binding between WSSV and the immobilized GST-WBP caused the capacitance to decrease ($C_{GST-WBP, WSSV}$) (ΔC_1). The regeneration solution (25 mM Gly–HCl, pH 2.40) was then injected to break the binding of the affinity binding pair, and the capacitance increased because of the higher ionic strength. The capacitance returned to the original baseline following a continuous flow of buffer, ready for a new analysis.

Table 1
Tested parameters and the optimum values of the flow injection capacitive biosensor for WSSV.

Parameters	Tested	Optimum
Regeneration solution		
Type	HCl, pH 2.40 25 mM Glycine–HCl, pH 2.40 NaOH, pH 9.00 25 mM $MgCl_2$	25 mM Glycine–HCl, pH 2.40
pH	2.20, 2.40, 2.60, 2.80	2.40
Concentration (mM)	10, 25, 50, 75, 100	25
Running buffer		
Tris–HCl buffer		
pH	7.00, 7.50, 7.80, 8.00, 8.20, 8.50	8.00
Concentration (mM)	10, 20, 25, 30, 50	25
Flow rate (μl/min)	25, 30, 50,70, 100	30
Sample volume (μl)	150, 250, 300, 500, 750	300

modified gold electrode after each immobilization step was examined by cyclic voltammetry (Eco Chemie μ-autolab B.V., Utrecht, Netherland) with 5 mM $K_3[Fe(CN)_6]$ in 0.1 M KCl between −0.3 and 0.7 V at a scan rate of 0.1 V/s vs. a Ag/AgCl electrode. A voltammogram of the cleaned gold surface showed the oxidation and reduction peaks (Fig. 3, curve a). Both peaks decreased when the SAM of thiourea was formed on the gold surface (Fig. 3, curve b). The insulating property of the electrode surface was further decreased when glutaraldehyde was reacted to thiourea and the GST-WBP was immobilized (Fig. 3, c and d, respectively). The modified electrode surface was then reacted with ethanolamine pH 8.50; this step was to occupy all the remaining aldehyde groups that had not coupled to the immobilized GST-WBP. Then the electrode surface was completely insulated by treatment with 1-dodecanethiol which was shown by the disappearance of the redox peaks (Fig. 3, curve e).

3.2. Optimization of the flow injection capacitive biosensor

The initial conditions used for the optimization of the flow injection capacitive biosensor were, running buffer 10 mM Tris–HCl buffer pH 7.00, flow rate 30 μl/min and sample volume 300 μl (100 copies/μl of standard WSSV in running buffer). When the optimum level of a parameter was obtained it was used for optimization of the following parameters.

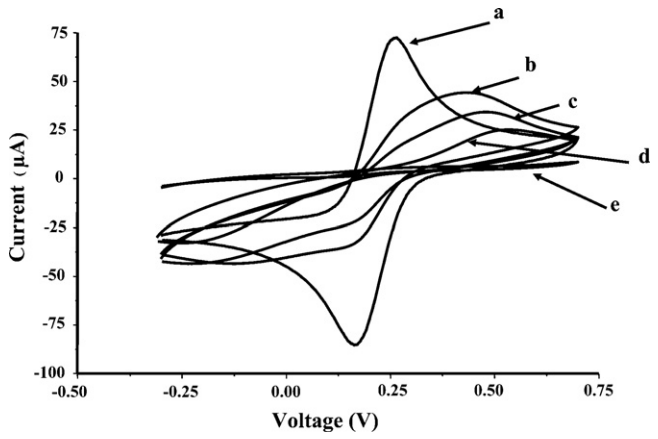

Fig. 3. Cyclic voltammograms of modified gold electrode with 5 mM $K_3[Fe(CN)_6]$ in 0.1 M KCl solution at a scan rate of 0.1 V/s vs. Ag/AgCl reference electrode, (a) clean gold electrode, (b) modified with SAM of thiourea, (c) activated by glutaraldehye, (d) immobilized GST-WBP and (e) blocking any pinholes on the electrode surface by 1-dodecanethiol.

3.2.1. Regeneration solution

When WSSV became bound to the immobilized GST-WBP on the electrode surface the capacitance decreased. After each analysis, WSSV needs to be removed to regenerate the electrode surface for a new measurement. The efficiency of the regeneration solution was determined by the residual activity calculated from the signal caused by the binding of GST-WBP to WSSV before (ΔC_1) and after (ΔC_2) regeneration (Fig. 2) as follows:

$$\text{Residual activity}\,(\%) = \frac{\Delta C_2 \times 100}{\Delta C_1} \quad (4)$$

Regenerating agents of low pH (25 mM glycine–HCl, pH 2.40 and HCl, pH 2.40), of high pH (NaOH, pH 9.00) and a high ionic strength agent (25 mM $MgCl_2$) were evaluated. The high pH reagent, gave the lowest residual activity (76 ± 12%). A higher residual activity was obtained from the high ionic strength reagent (87 ± 3%). The most effective was the low pH reagent where the HCl provided 93 ± 3% of residual activity and 97 ± 4% was obtained from the glycine–HCl reagent (Fig. 4(a)). Therefore, a pH of 2.20–2.80 of a 25 mM glycine–HCl reagent was further investigated. The highest residual activity was obtained using a pH of 2.40 (98 ± 2%) (Fig. 4(b)). Then the concentration (10–100 mM) at pH 2.40 was studied and the highest residual activity was obtained at 25 mM (97 ± 3%) (Fig. 4(c)). Therefore, 25 mM glycine–HCl at a pH of 2.40 was used as the optimal regeneration solution.

3.2.2. Running buffer

Tris–HCl buffer was used as the running buffer in the capacitive system because it provided a high capacitance change and a stable baseline for many analytes (Loyprasert et al., 2008; Numnuam et al., 2009; Suwansa-ard et al., 2009). Using 10 mM Tris–HCl buffer, the influence of pH (7.00–8.50) was investigated. The capacitance change increased with pH from 7.00 to 8.00 and then decreased. The maximum capacitance change was obtained at pH 8.00 (64 ± 4 nF/cm^2) (Fig. 5(a)). This is probably because the isoelectric point (p*I*) of the GST-WBP is 9.20 and the p*I* of the virus protein is 4.60 (Van Hulten et al., 2000, 2002). Therefore, at a pH of 8.00 GST-WBP had positive charge and WSSV had negative charge and this helped with the binding. Then the effect of Tris–HCl concentration (10–50 mM) at pH 8.00 was studied. The capacitance change increased with concentration, reaching a maximum at 25 mM (83 ± 4 nF/cm^2) and then decreased (Fig. 5(b)). Therefore, 25 mM Tris–HCl at a pH of 8.00 was used as the running buffer.

3.2.3. Flow rate

In a flow injection biosensor system, the flow rate was one of the factors to affect the yield of interaction between the affinity binding pair. Optimization of the flow rate (25–100 μl/min) was carried out by injecting 300 μl of 100 copies/μl of WSSV. The capacitance change increased when the flow rate decreased (Fig. 5(c)).

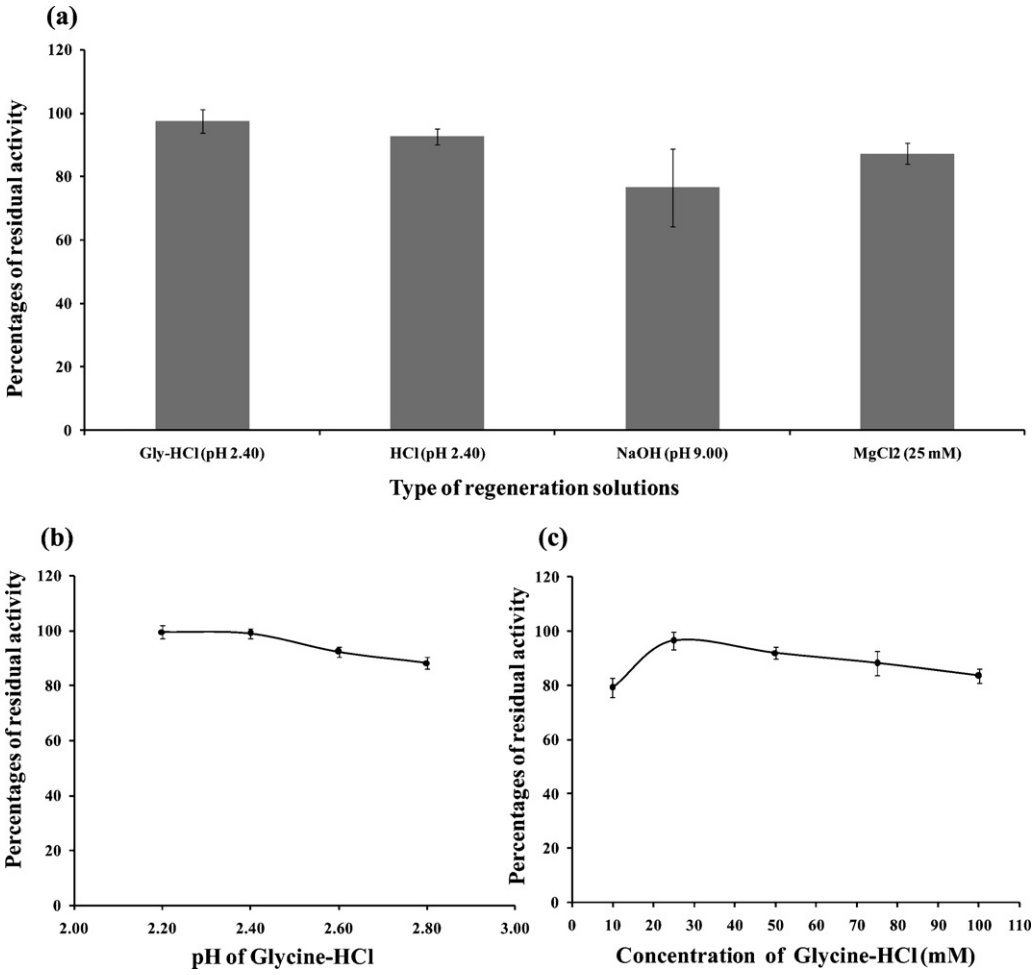

Fig. 4. Effects of various parameters of the regeneration solution on the percentages of residual activity (a) type; (b) pH of glycine–HCl, using 25 mM glycine–HCl; (c) concentration of glycine–HCl, using glycine–HCl, pH 2.40.

This is because a lower flow rate provided a longer contact time between the GST-WBP and WSSV. However, between the two lowest flow rates the capacitance change of 25 μl/min (84 ± 2 nF/cm^2) and 30 μl/min (83 ± 2 nF/cm^2) were not much different (1.3%) but the analysis time for 30 μl/min was shorter than for 25 μl/min (25 min compared to 30 min), therefore, the 30 μl/min was chosen.

3.2.4. Sample volume

The sample volume was studied between 150 and 750 μl. The capacitance change increased with sample volume up to 300 μl (82 ± 2 nF/cm^2) (Fig. 5(d)). After 300 μl the change in capacitance reached a maximum plateau. So, 300 μl was chosen because it can provide a high response and a short analysis time (25 min).

The optimal conditions are summarized in Table 1.

3.3. Linear dynamic range and detection limit

Standard WSSV solutions that ranged from 1 to 10^6 copies/μl were tested under optimum conditions (Table 1). The experiment was carried out in triplicate for each concentration. Fig. 6 shows examples of capacitance responses after injection of 1 copy/μl and 100 copies/μl of WSSV standard solutions compared to the blank (the running buffer). The capacitance response (ΔC) increased with the concentration. Although a small decrease of capacitance was detected after a blank injection, the response was always small compared to the ΔC when WSSV was injected. ΔC due to the blank solution also only lasted as long as the volume of the blank solution was passing through the sensing surface then the capacitance returned to its original baseline (Fig. 6 inset (a)). However, when WSSV was injected (followed by the running buffer) the capacitance decreased and remained at this new stable value (Fig. 6 inset (b)), until the regeneration solution was injected to break the binding between the immobilized GST-WBP and the WSSV. Fig. 7(a) shows the calibration plot for WSSV. A linear relationship between the capacitance change and the logarithm of WSSV concentration was obtained from 1 to 10^5 copies/μl ($r = 0.9957$). The detection limit was 1 copy/μl, based on the IUPAC Recommendation 1994 (Buck and Lindner, 1994).

3.4. Reproducibility

Reproducibility was investigated at optimum conditions by continuously detecting the change of capacitance at the same concentration of standard WSSV (100 copies/μl) with subsequent regeneration after each measurement to remove WSSV from the immobilized GST-WBP on the electrode. The capacitance change after regeneration was used to calculate the percentage residual activity of GST-WBP by comparing the response to the initial capacitance change. The average residual activity of the first 39 analysis cycles was $95.8 \pm 2.3\%$ after which the residual activity dropped below 90%. That is, the modified electrode can be regenerated and reused with good reproducibility for up to 39 times (RSD = 2.4%). The electrode was tested by cyclic voltammetry after being used. The voltammogram was similar to the one obtained before the elec-

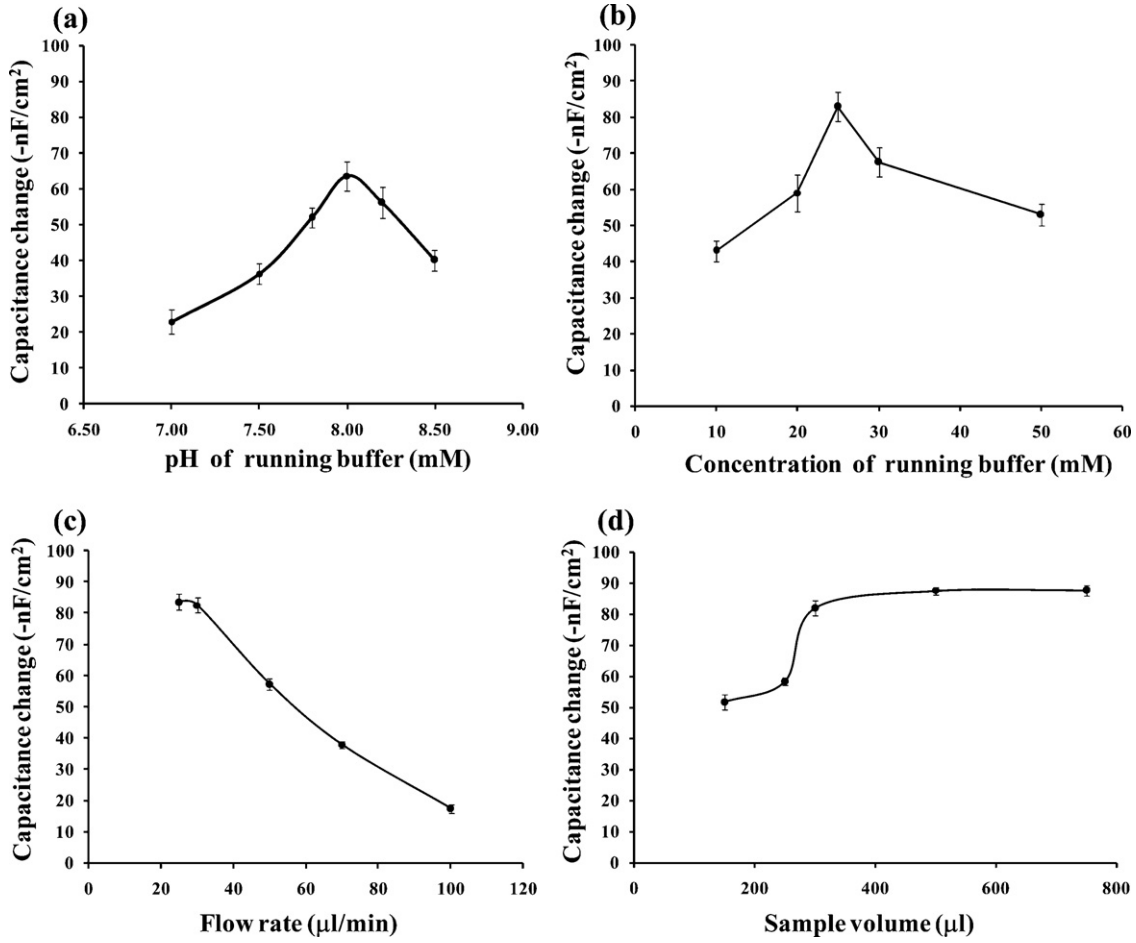

Fig. 5. Effects of the flow parameters on the response affinity biosensor to (a) pH of the running buffer, using 10 mM Tris–HCl at different pH values at the flow rate of 30 μl/min and a sample volume of 300 μl; (b) running buffer concentration, using different concentrations of Tris–HCl, pH 8.00 at the flow rate of 30 μl/min and a sample volume of 300 μl; (c) flow rate, using 25 mM Tris–HCl, pH 8.00 at different flow rates; (d) sample volume, using 25 mM Tris–HCl, pH 8.00 at the flow rate of 30 μl/min and different sample volumes.

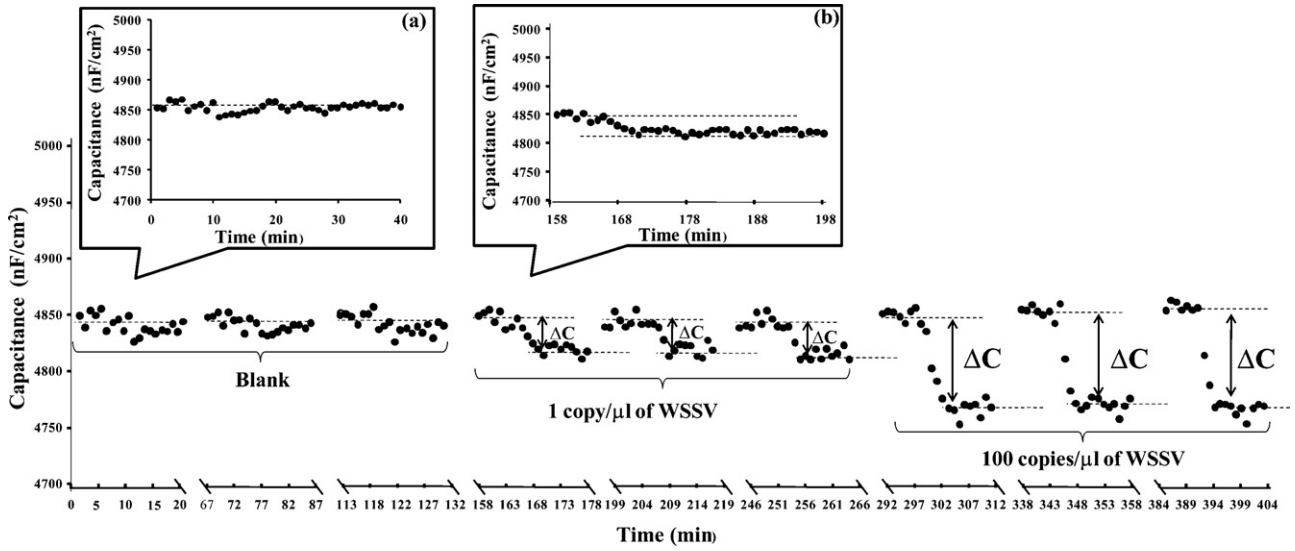

Fig. 6. Examples of capacitance responses of WSSV (300 μl) at 1 and 100 copies/μl compared to a blank (the running buffer without WSSV). Inset (a) a small decrease of capacitance was detected after blank injection then the capacitance returned to the original baseline after the volume of blank solution passed through the sensing surface. Inset (b) when WSSV was injected (followed by the running buffer) the capacitance decreased and remained at this new stable value.

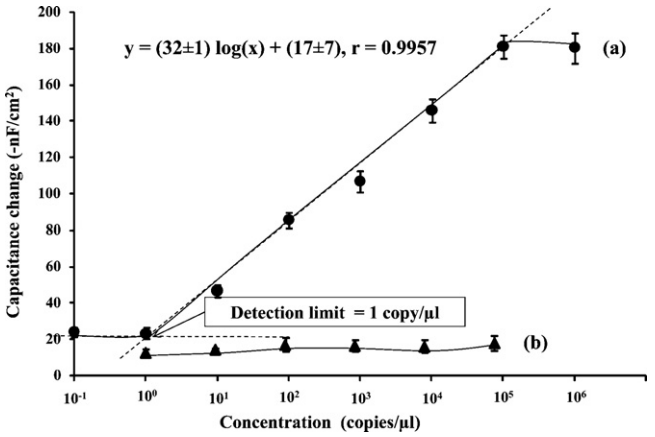

Fig. 7. Calibration plot of the white spot syndrome virus (WSSV) was obtained from the flow injection capacitive biosensor under optimum conditions showing a linear range between 1 and 10^5 copies/μl and a detection limit at 1 copy/μl (a). Capacitance change vs. concentration of yellow head virus (YHV) (b).

trode was used, i.e. no redox peaks were observed (Fig. 3e). That is, the decrease in the residual activity was not due to the loss of the self-assembled monolayer but probably caused by the loss of either the GST-WBP or its activity.

3.5. Selectivity

Yellow head virus (YHV) was used to test the selectivity of the capacitive biosensor system. At the same concentration range (1–10^5 copies/μl), YHV gave a very low response compared to WSSV (Fig. 7(b)), and much lower than the response at the detection limit of WSSV. That is, the proposed method provided a high specificity for detecting WSSV.

3.6. Matrix interference

High amounts of salt in real water samples can affect the capacitance response. One method to reduce this effect is by dilution. However, WSSV in water needs to be detected at low concentration so dilution is not a realistic option. The effect of salt can also be reduced by a desalting process using desalt columns (BIO-RAD, Hercules, CA, USA). After this process salt was retained in the column and the sample passed through. The influence of salts and other matrix interferences present in real water sample were first studied. A real water sample from a shrimp pond was filtered by a filter membrane (pore size 0.2 μm, Millipore, Bedford, USA) to remove WSSV that might come with the water (Esparza-Leal et al., 2009). Then it was spiked with 4 different concentrations of WSSV (1, 25, 50 and 100 copies/μl) followed by the desalting process. The conductance of the water was measured (Conductivity Meter 4310, Jenway, Staffordshire, UK) after the desalting process. The process was repeated until the conductance of the real water sample was similar to that of the running buffer (300–330 μS), the number of repeats depended on each water sample. The four spiked desalted water samples were then injected into the capacitive system and the responses were plotted vs. concentration. This was the "matrix matched calibration plot". The "standard calibration plot" (using a standard solution of WSSV in running buffer) was also obtained at the same concentration of WSSV. The slopes of both calibration plots were compared using two-way ANOVA, calculated by R software (R Development Core Team, 2006) to test whether or not they differ significantly. The slopes of the two calibration plots showed significant differences ($P > 0.05$). That is, the matrix has some effect on the response. Therefore, for real water analysis a matrix matched calibration plot was prepared and used to determine the WSSV concentration in the real water samples (Eurachem, 1998).

3.7. Recovery

To test the matrix matched calibration, recovery of the spiked samples were investigated. A filtered real water sample (pore size 0.2 μm, Millipore, Bedford, USA) was used to prepare the spiked WSSV standards (1, 25, 50, 100 copies/μl). The spiked samples were desalted and analyzed by the capacitive system to obtain the matrix match calibration plot. The filtered water was also spiked to obtain 10 and 75 copies/μl of testing solution of the WSSV. These were also desalted before being injected into the capacitive system. Capacitance changes were obtained for these two tested solutions. These were used to calculate the WSSV concentrations from the matrix match calibration plot. The concentrations obtained were 9.3 ± 0.5 and 72 ± 2 copies/μl. That is, the percentage recovery of 10 and 75 copies/μl were 93 ± 5 and $97 \pm 3\%$ respectively. Therefore, the matrix matched calibration can be used to determine WSSV in water sample. Filtered water that has been desalted was also injected and tested as a control. The obtained signal was very low and only calculated to be 0.08 ± 0.07 copy/μl.

To further validate the method, recoveries were studied for all eight real samples. A matrix match calibration plot for each sample was first prepared as described above. Then the spiked samples (1, 25, 50 and 100 copies/μl) were desalted and analyzed by the capacitive biosensor. The concentrations of WSSV were determined from the matrix match calibration plots. The results showed average recoveries between 68 and 127% with a relative standard deviation (RSD) of between 3 and 19% (Table 2).

3.8. Real sample analysis

Each of the shrimp pond water samples (see Section 2.5) were divided into two portions. One portion was filtered to remove the existing virus, spiked with WSSV to obtain the concentrations between 1 and 100 copies/μl, treated with desalting columns and used to prepare the matrix matched calibration plot. The other portion was treated with a desalting column and then analyzed. The obtained capacitance change ($-nF/cm^2$) was used to determine the WSSV concentration from the matrix matched calibration plot. The results from the eight samples are shown in Table 3.

To validate the method, all samples were tested with real-time PCR (Table 3). Comparison between the two analysis techniques (samples 1–4 and 7–8, Table 3) was done by the Wilcoxon signed rank test. The results indicated that there was no evidence of systematic differences between the results obtained from the capacitive biosensor system and real-time PCR ($P > 0.05$). That is, the concentrations determined by the flow injection capacitive biosensor and real-time PCR are in good agreement.

4. Discussion

This project has shown that the proposed capacitive biosensor is a highly sensitive method for the quantitative detection of WSSV in shrimp pond water samples. Under optimum conditions, the capacitive biosensor provided linearity that ranged from 1 to 1×10^5 copies/μl, was rapid (20–25 min), had a high selectivity to a real time PCR WSSV analysis, and an extremely low detection limit of 1 copy/μl. The proposed biosensor provided a much better detection limit than other methods such as real-time PCR that gave a detection limit of 20 copies/μl (Srisala et al., 2008), PCR combined with an immunological method had a detection limit of 160 copies/μl in shrimp tissue samples (Srisala et al., 2008) and an RT-LAMP method had a detection limit of 100 copies/μl in

Table 2
Recoveries of spiked shrimp pond water samples ($n = 3$).

Shrimp pond water samples	% Recovery							
	Spiked concentration (copies/μl)							
	1		25		50		100	
	Determined concentration	% Recovery	Determined concentration	% Recovery	Determined concentration	% Recovery	Determined concentration	% Recovery
Sample 1	1.27 ± 0.11	127 ± 11	22.1 ± 3.8	88 ± 14	50.2 ± 6.6	100 ± 13	99.4 ± 7.6	99 ± 8
Sample 2	1.23 ± 0.19	123 ± 19	24.4 ± 1.5	98 ± 6	54.8 ± 8.3	110 ± 17	100.3 ± 3.4	100 ± 3
Sample 3	0.95 ± 0.11	95 ± 11	25.0 ± 4.8	100 ± 19	48.0 ± 7.2	96 ± 14	101.8 ± 2.9	102 ± 3
Sample 4	1.17 ± 0.09	117 ± 9	23.7 ± 2.0	95 ± 8	54.4 ± 8.1	109 ± 16	100.0 ± 5.2	100 ± 5
Sample 5	1.27 ± 0.13	127 ± 13	24.6 ± 1.7	98 ± 7	44.5 ± 5.6	89 ± 11	101.2 ± 5.3	101 ± 5
Sample 6	1.14 ± 0.10	114 ± 10	20.4 ± 2.1	82 ± 8	46.7 ± 3.7	93 ± 7	97.8 ± 3.0	98 ± 3
Sample 7	0.99 ± 0.12	99 ± 12	22.8 ± 3.0	91 ± 12	53.7 ± 6.7	107 ± 13	102.9 ± 2.7	103 ± 3
Sample 8	0.68 ± 0.12	68 ± 12	26.8 ± 3.4	107 ± 14	48.1 ± 5.4	96 ± 11	100.5 ± 5.6	101 ± 6

Table 3
Comparison of WSSV concentrations in shrimp pond water samples obtained from the flow injection capacitive biosensor system (mean ± SD, $n = 3$) and real time polymerase chain reaction.

Shrimp pond water samples	WSSV founded (copies/μl)	
	Capacitance system	Real-time PCR
Sample 1	839 ± 4	837
Sample 2	674 ± 2	673
Sample 3	66 ± 2	65
Sample 4	56 ± 5	58
Sample 5	5 ± 1	ND
Sample 6	7 ± 1	ND
Sample 7	15 ± 4	19
Sample 8	56 ± 4	54

ND, not detectable.

shrimp tissue samples (Mekata et al., 2009). Therefore, the proposed biosensor offers a promising alternative for the detection of WSSV in water at trace amount. This will prevent the use of WSSV contaminated pond water before pond stocking and could monitor the spread of WSSV during shrimp cultivation. In addition, the biorecognition element (GST-WBP) is specific to WSSV. With this method the analysis cost can be reduced since the modified electrode can be reused up to 39 times by using the appropriate regenerating solution.

The proposed biosensor is highly selective to WSSV when compared with YHV. This is because the detected capacitance signal was caused by the binding between immobilized GST-WBP and WSSV through protein–protein binding mechanisms. Since WSSV and YHV contain different major proteins, i.e. YHV contains three major proteins (110–135 kDa, 63–67 kDa and 20–22 kDa) (Cowley et al., 2004; Assavalapsakul et al., 2005) and WSSV contains four major proteins (15 kDa, 19 kDa, 26 kDa and 28 kDa) (Van Hulten et al., 2000; Tang et al., 2007) and the WBP can bind specifically to the VP26 (26 kDa) protein of WSSV (Youtong et al., 2011) so the presence of YHV would not interfere with WSSV detection. In addition, VP26 of WSSV has a unique structure that is not observed in other viral proteins (Tang et al., 2007) therefore this system should be very specific to WSSV.

All water samples showed significant differences between standard and matrix matched calibration plots. That is, the matrix has some effect on the WSSV analysis. Thus, the matrix matched calibration plot is needed for WSSV calculation in water samples. The proposed biosensor, when applied to detect WSSV in shrimp pond water samples provided the same result compared to real-time PCR ($P > 0.05$). One of the main advantages of the proposed biosensor over the real-time PCR was the extremely low detection limit, 1 copy/μl, making it possible to detect lower amounts of WSSV. This can be seen clearly in samples 5 and 6 (Table 3) where the low detection limit of the capacitive biosensor allowed quantitative determination of 5 ± 1 and 7 ± 1 copies/μl respectively, while they were not detectable with real-time PCR (detection limit 20 copies/μl) (Srisala et al., 2008). This proposed biosensor system can certainly be applied to detect other viruses using biorecognition elements specific to each virus.

Acknowledgements

The authors are grateful for support from The Royal Golden Jubilee PhD-Program (RGJ) supported by the Thailand Research Fund; Center for Innovation in Chemistry: Postgraduate Education and Research Program in Chemistry (PERCH-CIC); the National Research University Project of Thailand, the office of the Higher Education Commission; Trace Analysis and Biosensor Research Center (TAB-RC), the Graduate School and the Faculty of Science, Prince of Songkla University, Hat Yai, Songkhla, Thailand. The authors also thank Prof. Bo. Mattiasson, Department of Biotechnology, Lund University, Box 124, Lund, Sweden for the idea of using the VP26 protein to detect viruses. The authors also thank Dr. Brian Hodgson, Prince of Songkla University, Hat Yai, Songkhla, Thailand for the English assistance with the manuscript.

References

Assavalapsakul, W., Tirasophon, W., Panyim, S., 2005. Antiserum to the gp116 glycoprotein of yellow head virus neutralizes infectivity in primary lymphoid organ cells of *Penaeus monodon*. Dis. Aquat. Org. 63, 85–88.
Bard, A.J., Faulkner, L.R., 2001. Electrochemical Methods: Fundamentals and Applications, 2nd ed. John Wiley & Sons, Inc., New York.
Berggren, C., Bjarnason, B., Johansson, G., 2001. Capacitive biosensors. Electroanalysis 133, 173–180.
Berggren, C., Johansson, G., 1997. Capacitance measurements of antibody–antigen interactions in a flow system. Anal. Chem. 69, 3651–3657.
Bontidean, I., Berggren, C., Johansson, G., Csoregi, E., Mattiasson, B., Lloyd, J.R., Jakeman, K.J., Brown, N.L., 1998. Detection of heavy metal ions at femtomolar levels using protein-based biosensor. Anal. Chem. 70, 4162–4169.

Buck, R.P., Lindner, E., 1994. Recommendations for nomenclature of ion-selective electrodes (IUPAC Recommendations 1994). Pure Appl. Chem., 2527–2536.
Chen, Z.J., Wang, C.S., Shih, H.H., 2002. An assay for quantification of white spot syndrome virus using a capture ELISA. J. Fish Dis. 25, 249–251.
Cohen, J.M., Samocha, T.M., Fox, J.M., Gandy, R.L., Lawrence, A.L., 2005. Characterization of water quality factors during intensive raceway production of juvenile *Litopenaeus vanamei* using limited discharge and biosecure management tools. Aquat. Eng. 32, 425–442.
Cowley, J.A., Cadogan, L.C., Spann, K.M., Sittidilokratna, N., Walker, P.J., 2004. The gene encoding the nucleocapsid protein of gill-associated nidovirus of *Penaeus monodon* prawns is located upstream of the glycoprotein gene. J. Virol. 78, 8935–8941.
Dhar, A.K., Roux, M.M., Klimpel, K.R., 2001. Detection and quantification of infectious hypodermal and hematopoietic necrosis virus and white spot virus in shrimp using real-time quantitative PCR and SYBR green chemistry. J. Clin. Microbiol. 39, 2835–2845.
Eurachem Guide, 1998. The fitness for purpose of analytical methods: a laboratory guide to method validation and related topics.
Esparza-Leal, H.M., Escobedo-Bonilla, C.M., Casillas-Hernández, R., Álvarez-Ruíz, P., Portillo-Clark, G., Valerio-García, R.C., Hernández-López, J., Méndez-Lozano, J., Vibanco-Pérez, N., Magallón-Barajas, F.J., 2009. Detection of white spot syndrome virus in filtered shrimp-farm water fractions and experiment evaluation of its infectivity in *Penaeus* (*Litopenaeus*) *vannamei*. Aquaculture 292, 16–22.
Flegel, T.W., 2006. The special danger of viral pathogens in shrimp translocated for aquaculture. Sci. Asia 32, 215–221.
Gebbert, A., Alvarez-Icaza, M., Stoecklein, W., Schmid, R.D., 1992. Real-time monitoring of immunochemical interactions with a tantalum capacitance flow-through cell. Anal. Chem. 64, 997–1003.
Hameed, A.S.S., Parameswaran, V., Musthaq, S.S., Sudhakaran, R., Balasubramanian, G., Yoganandhan, K., 2005. A simple PCR procedure to detect white spot syndrome virus (WSSV) of shrimp, *Penaeus monodon* (Fabricius). Aquacult. Int. 13, 441–450.
Hedstrom, M., Galaev, I.Y., Mattiasson, B., 2005. Continuous measurements of a binding reaction using a capacitive biosensor. Biosens. Bioelectron. 21, 41–48.
Hossain, Md.S., Chakraborty, A., Joseph, B., Otta, S.K., Karunasagar, I., Karunasagar, I., 2001. Detection of new hosts for white spot syndrome virus of shrimp using nested polymerase chain reaction. Aquaculture 198, 1–11.
Hossain, Md.S., Otta, S.K., Chakraborty, A., Kumar, H.S., Karunasagar, I., Karunasagar, I., 2004. Detection of WSSV in cultured shrimps, captured brooders, shrimp postlarvae and water samples in Bangladesh by PCR using different primers. Aquaculture 237, 59–71.
Jiang, D., Tang, J., Liu, B., Yang, P., Shen, X., Kong, J., 2003. Covalently coupling the antibody on an amine-self-assembled gold surface to probe hyaluronan-binding protein with capacitance measurement. Biosens. Bioelectron. 18, 1183–1191.
Kono, T., Savan, R., Sakai, M., Itami, T., 2004. Detection of white spot syndrome virus in shrimp by loop-mediated isothermal amplification. J. Virol. Methods 115, 59–65.
Lightner, D.V. (Ed.), 1996. A Handbook of Shrimp Pathology and Diagnostic Procedures for Diseases of Cultured Penaeid Shrimp. World Aquaculture Society, Baton Rouge, LA, USA.
Lightner, D.V., 2005. Biosecurity in shrimp farming: pathogen exclusion through use of SPF stock and routine surveillance. J. World Aquacult. Soc. 36, 229–248.
Limbut, W., Kanatharana, P., Mattiasson, B., Asawatreratanakul, P., Thavarungkul, P., 2006. A comparative study of capacitive immunosensors based on self-assembled monolayers formed from thiourea, thioctic acid and 3-mercaptopropionic acid. Biosens. Bioelectron. 22, 233–240.
Lo, C.F., Leu, J.H., Ho, C.H., Chen, C.H., Peng, S.E., Chen, Y.T., Chou, C.M., Yeh, P.Y., Huang, C.J., Chou, Y.H., Wang, C.H., Kou, G.H., 1996. Detection of baculovirus associated with white spot syndrome (WSBV) in penaeid shrimps using polymerase chain reaction. Dis. Aquat. Org. 25, 133–141.
Loyprasert, S., Thavarungkul, P., Asawatreratanakul, P., Wongkittisuksa, B., Limsakul, C., Kanatharana, P., 2008. Label-free capacitive immunosensor for microcystin-LR using self-assembled thiourea monolayer incorporated with Ag nanoparticles on gold electrode. Biosens. Bioelectron. 24, 78–86.
Mekata, T., Sudhakaran, R., Kono, T., Supamattaya, K., Linh, N.T.H., Sakai, M., Itami, T., 2009. Real-time quantitative loop-mediated isothermal amplification as a simple method for detecting white spot syndrome virus. Lett. Appl. Microbiol. 48, 25–32.
Mirsky, V.M., Riepl, M., Wolfbeis, O., 1997. Capacitive monitoring of protein immobilization and antigen–antibody reactions on monomolecular alkylthiol films on gold electrodes. Biosens. Bioelectron. 12, 977–989.
Natividad, K.D.T., Nomura, N., Matsumura, M., 2008. Detection of white spot syndrome virus DNA in pond soil using a 2-step nested PCR. J. Virol. Methods 149, 28–34.
Numnuam, A., Kanatharana, P., Mattiasson, B., Asawatreratanakul, P., Wongkittisuksa, B., Limsakul, C., Thavarungkul, P., 2009. Capacitive biosensor for quantification of trace amounts of DNA. Biosens. Bioelectron. 24, 2559–2565.
Quang, N., Hoa, T., Da, T., Anh, P., 2009. Persistence of white spot syndrome virus in shrimp ponds and surrounding areas after an outbreak. Environ. Monit. Assess. 156, 69–72.
R Development Core Team, 2006. R: A language and environment for statistical computing. R Foundation for Statistical Computing, Vienna, Austria. ISBN 3-900051r-r07-0.
Rajendran, K.V., Vijayan, K.K., Santiago, T.C., Rajan, J.J.S., 2005. White spot syndrome virus (WSSV) infection in tiger shrimp *Penaeus monodon*: a non-lethal histopathological rapid diagnostic method using paraffin and frozen sections. Aquacult. Int. 13, 341–349.
Srisala, J., Tacon, P., Flegel, T.W., Sritunyalucksana, K., 2008. Comparison of white spot syndrome virus PCR-detection methods that use electrophoresis or antibody-mediated lateral flow chromatographic strips to visualize PCR amplicons. J. Virol. Methods 153, 129–133.
Sritunyalucksana, K., Srisala, J., McColl, K., Nielsen, L., Flegel, T.W., 2006. Comparison of PCR testing methods for white spot syndrome virus (WSSV) infections in penaeid shrimp. Aquaculture 25, 95–104.
Suwansa-ard, S., Kanatharana, P., Asawatreratanakul, P., Wongkittisuksa, B., Limsakul, C., Thavarungkul, P., 2009. Comparison of surface plasmon resonance and capacitive immunosensors for cancer antigen 125 detection in human serum samples. Biosens. Bioelectron. 24, 3436–3441.
Tan, L.T., Soon, S., Lee, K.L., Shariff, M., Hassan, M.D., Omar, A.R., 2001. Quantitative analysis of an experimental white spot syndrome virus (WSSV) infection in *Penaeus monodon* Fabricius using competitive polymerase chain reaction. J. Fish Dis. 24, 315–323.
Tang, X., Wu, J., Sivaraman, J., Hew, C.L., 2007. Crystal structures of major envelope protein VP26 and VP28 from white spot syndrome virus shed light on their evolutionary relationship. J. Virol. 81, 6709–6717.
Tanticharoen, M., 2008. Aquacultural biotechnology in Thailand: the case of the shrimp industry. Int. J. Biotechnol. 10, 588–603.
Van Hulten, M.C.W., Reijns, M., Vermeesch, A.M.G., Zandbegen, F., Valk, J.M., 2002. Identification of VP19 and VP15 of white spot syndrome virus (WSSV) and glycosylation status of the WSSV major structural proteins. J. Gen. Virol. 83, 257–265.
Van Hulten, M.C.W., Goldbach, R.W., Vlak, J.M., 2000. Three functionally diverged major structural proteins of white spot syndrome virus enveloped by gene duplication. J. Gen. Virol. 81, 2525–2529.
Wang, X., Zhan, W., 2006. Development of an immunochromatographic test to detect White Spot Syndrome Virus of shrimp. Aquaculture 255, 196–200.
Wongkittisuksa, B., Limskul, C., Kanatharana, P., Limbut, W., Asawatreratanakul, P., Dawan, S., Loyprasert, S., Thavarungkul, P., 2011. Development and application of a real-time capacitive sensor. Biosens. Bioelectron. 26, 2466–2472.
Youtong, W., Deachamag, P., Phongdara, A., Chotigeat, W., 2011. WSSV: VP26 binding proteins and its biological activity. Fish Shellfish Immunol. 30, 77–83.
Yuan, L., Zhang, X., Chang, M., Jia, C., Hemmingsen, S.M., Dai, H., 2007. A new fluorescent quantitative PCR-based in vitro neutralization assay for white spot syndrome virus. J. Virol. Methods 146, 96–103.